

## Electronic Spectrum of Propadienylidene ( $\text{H}_2\text{C}=\text{C}=\text{C}:$ )

John F. Stanton\*

Institute for Theoretical Chemistry  
Departments of Chemistry and Biochemistry  
The University of Texas at Austin  
Austin, Texas 78712

Jeffrey T. DePinto, Randal A. Seburg,  
Jonathan A. Hodges, and Robert J. McMahon\*

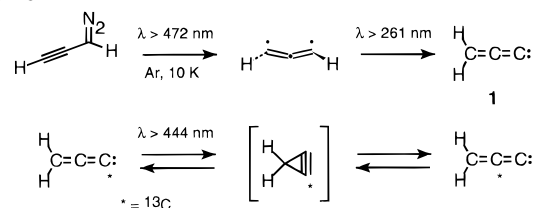
Department of Chemistry, University of Wisconsin  
1101 University Avenue, Madison, Wisconsin 53706

Received June 6, 1996

The carbenes  $\text{H}_2\text{C}(\text{=C})_n$  ( $n = 0, 1, 2, \dots$ ) comprise a fundamentally important series of molecules. Each of the first three members represents a paradigm in chemistry. The simplest carbene is methylene ( $\text{H}_2\text{C}:$ ),<sup>1</sup> while vinylidene ( $\text{H}_2\text{C}=\text{C}:$ ) teeters on the edge of existence because it rapidly rearranges to acetylene.<sup>2</sup> Propadienylidene ( $\text{H}_2\text{C}=\text{C}=\text{C}:$ ) (**1**) is the first member of the higher homologs to exhibit greater stability. Indeed, both propadienylidene<sup>3</sup> and butatrienylidene<sup>4</sup> have been detected in interstellar clouds by microwave radioastronomy. Recent interest in propadienylidene also stems from studies that implicate this species as a key intermediate in thermal and photochemical rearrangements of  $\text{C}_3\text{H}_2$  isomers.<sup>5,6</sup> Previous theoretical investigations provide reliable insight into the ground state structure of propadienylidene and higher homologs,<sup>7</sup> but little is known about the excited states of these species. To our knowledge, the only detection of an excited state of propadienylidene comes from a photodetachment study<sup>8</sup> in which the  $^3B_1$  state was located 1.29 eV above the ground state of the neutral species. However, nothing is known about the singlet excited states that are most easily accessed by photon absorption. The striking photochemical automerization of  $^{13}\text{C}$ -labeled propadienylidene<sup>6</sup> (Scheme 1) induced us to explore the excited states of **1** in greater detail. We now report the first electronic absorption spectrum of propadienylidene and its assignment, which is based on high-level *ab initio* calculations.

Long-wavelength photolysis ( $\lambda > 472$  nm) of diazopropyne, matrix isolated in argon at 10 K, yields triplet propynylidene.<sup>9</sup> Subsequent short-wavelength irradiation ( $\lambda > 261$  nm) causes the IR, UV/vis, and ESR signals of triplet propynylidene to disappear and the IR<sup>5,6</sup> and UV/vis absorptions of singlet propa-

### Scheme 1



dienylidene (**1**) to appear. The electronic spectrum of **1** (Figure 1) exhibits rich vibronic structure with absorption maxima that span virtually the entire visible spectrum.<sup>10</sup> Given the density of features in the visible region, it is enticing to speculate that the family of  $\text{H}_2\text{C}(\text{=C})_n$  carbenes may be responsible for some of the mysterious “diffuse interstellar bands”.<sup>11</sup>

To aid in interpreting the electronic spectrum of **1**, its three lowest singlet excited states have been characterized with the equation-of-motion coupled-cluster method in the singles and doubles approximation (EOMEE-CCSD)<sup>12</sup> using a local version of the ACES II program system.<sup>13</sup> Excitation energies calculated with EOMEE-CCSD<sup>14</sup> tend to be systematically too high, but the magnitude of the discrepancy is typically less than 0.5 eV.<sup>15</sup> For polyatomic molecules, the formulation and implementation of an efficient analytic energy derivative procedure for EOMEE-CCSD<sup>16</sup> is essential for calculating the properties of interest in this research (adiabatic excitation energies and final state vibrational frequencies).<sup>17</sup>

Equilibrium geometries and harmonic vibrational frequencies for the ground state of **1** and the three lowest excited states ( $\tilde{A}^1A_2$ ,  $\tilde{B}^1B_1$ , and  $\tilde{C}^1A_1$ ) were obtained with a triple- $\zeta$  plus double polarization (TZ2P)<sup>18</sup> basis set; the corresponding adiabatic excitation energies are given in Table 1.<sup>19</sup>

The larger cc-pVTZ and cc-pVQZ basis sets<sup>20</sup> have been used to explore the sensitivity of excitation energies to further improvement of the basis. Electronic (vibrationless) energy differences were calculated with these basis sets at the optimized TZ2P geometries and augmented by zero-point vibrational energies calculated from the TZ2P harmonic frequencies; the results of these calculations are listed in Table 1. Expansion of the basis from the TZ2P set to cc-pVQZ leads to larger excitation energies for all three states, but the magnitude of the difference is less than  $1000\text{ cm}^{-1}$  in all cases. Given the relative insensitivity of excitation energies with respect to the choice of basis set, it is likely that all of the cc-pVQZ results listed in

- (1) Schaefer, H. F. *Science* **1986**, 231, 1100.  
(2) Stanton, J. F.; Gauss, J. *J. Chem. Phys.* **1994**, 101, 3001 and references therein.  
(3) (a) Vrtilek, J. M.; Gottlieb, C. A.; Gottlieb, E. W.; Killian, T. C.; Thaddeus, P. *Astrophys. J.* **1990**, 364, L53. (b) Cernicharo, J.; Gottlieb, C. A.; Guélin, M.; Killian, T. C.; Paubert, G.; Thaddeus, P.; Vrtilek, J. M. *Astrophys. J.* **1991**, 368, L39.  
(4) (a) Killian, T. C.; Vrtilek, J. M.; Gottlieb, C. A.; Gottlieb, E. W.; Thaddeus, P. *Astrophys. J.* **1990**, 365, L89. (b) Cernicharo, J.; Gottlieb, C. A.; Guélin, M.; Killian, T. C.; Thaddeus, P.; Vrtilek, J. M. *Astrophys. J.* **1991**, 368, L43.  
(5) Maier, G.; Reisenauer, H.-P.; Schwab, W.; Čársky, P.; Hess, B. A., Jr.; Schaad, L. J. *J. Am. Chem. Soc.* **1987**, 109, 5183.  
(6) Seburg, R. A.; McMahon, R. J. *Angew. Chem.* **1995**, 107, 2198; *Angew. Chem., Int. Ed. Engl.* **1995**, 34, 2009.  
(7) (a) Gottlieb, C. A.; Killian, T. C.; Thaddeus, P.; Botschwina, P.; Flügge, J.; Oswald, M. J. *J. Chem. Phys.* **1993**, 98, 4478. (b) Maluendes, S. A.; McLean, A. D. *Chem. Phys. Lett.* **1992**, 200, 511. (c) Jonas, V.; Böhme, M.; Frenking, G. *J. Phys. Chem.* **1992**, 96, 1640. (d) Cooper D. L.; Murphy, S. C. *Astrophys. J.* **1988**, 333, 482. (e) DeFrees, D. J.; McLean, A. D. *Astrophys. J.* **1986**, 308, L31. (f) Dykstra, C. E.; Parsons, C. A.; Oates, C. L. *J. Am. Chem. Soc.* **1979**, 101, 1962. (g) Kenney, J. W.; Simons, J.; Purvis, G. D.; Bartlett, R. J. *J. Am. Chem. Soc.* **1978**, 100, 6930. (h) Hehre, W. J.; Pople, J. A.; Lathan, W. A.; Radom, L.; Wasserman, E.; Wasserman, Z. R. *J. Am. Chem. Soc.* **1976**, 98, 4378.  
(8) Robinson, M. S.; Polak, M. L.; Bierbaum, V. M.; DePuy, C. H.; Lineberger, W. C. *J. Am. Chem. Soc.* **1995**, 117, 6766.  
(9) Seburg, R. A.; DePinto, J. T.; Patterson, E. V.; McMahon, R. J. *J. Am. Chem. Soc.* **1995**, 117, 835.

- (10) UV/vis (Ar, 10 K)  $\lambda_{\text{max}}$  (in nm) 717, 707, 695, 682, 666, 646, 639, 628, 618, 607, 602, 590, 572, 565, 535, 508, 480, 458, 436, 418, 400, 382, 270, 259, 252, 246, 240, 236, 231, 227, 222, 218, 213.  
(11) For a leading reference, see: *The Diffuse Interstellar Bands*; Tielens, A. G. G. M., Snow, T. P., Eds.; Kluwer: Dordrecht, 1995.  
(12) Stanton, J. F.; Bartlett, R. J. *J. Chem. Phys.* **1993**, 98, 7029 and references therein.  
(13) Stanton, J. F.; Gauss, J.; Watts, J. D.; Lauderdale, W. J.; Bartlett, R. J. *Int. J. Quantum Chem.* **1991**, S182, 207.  
(14) For reviews of coupled-cluster theory, see: Bartlett, R. J. *J. Phys. Chem.* **1989**, 93, 1697. Lee, T. J.; Scuseria, G. E. In *Quantum Mechanical Electronic Structure Calculations with Chemical Accuracy*; Langhoff, S. R., Ed.; Kluwer Academic: Dordrecht, 1995; p 47.  
(15) See, for example: Stanton, J. F.; Gauss, J.; Ishikawa, N.; Head-Gordon, M. *J. Chem. Phys.* **1994**, 103, 4160 and also in ref 12.  
(16) Stanton, J. F. *J. Chem. Phys.* **1993**, 99, 8840. Stanton, J. F.; Gauss, J. *J. Chem. Phys.* **1994**, 100, 4695.  
(17) Stanton, J. F.; Gauss, J. *J. Chem. Phys.* In press.  
(18) The TZ2P basis for C and H comprises the 5s3p and 3s contracted sets of Dunning [Dunning, T. H. *J. Chem. Phys.* **1971**, 55, 716] augmented by polarization functions described in: Gauss, J.; Stanton, J. F.; Bartlett, R. J. *J. Chem. Phys.* **1992**, 97, 7825.  
(19) Calculations for the electronic ground state were carried out with the coupled-cluster singles and doubles method [Purvis, G. D.; Bartlett, R. J. *J. Chem. Phys.* **1982**, 76, 1910], while the EOMEE-CCSD approximation was used for the excited states. Only the pure spherical harmonic components of d, f, and g-type Gaussian basis functions have been retained in the calculations.  
(20) Dunning, T. H. *J. Chem. Phys.* **1989**, 90, 1007.

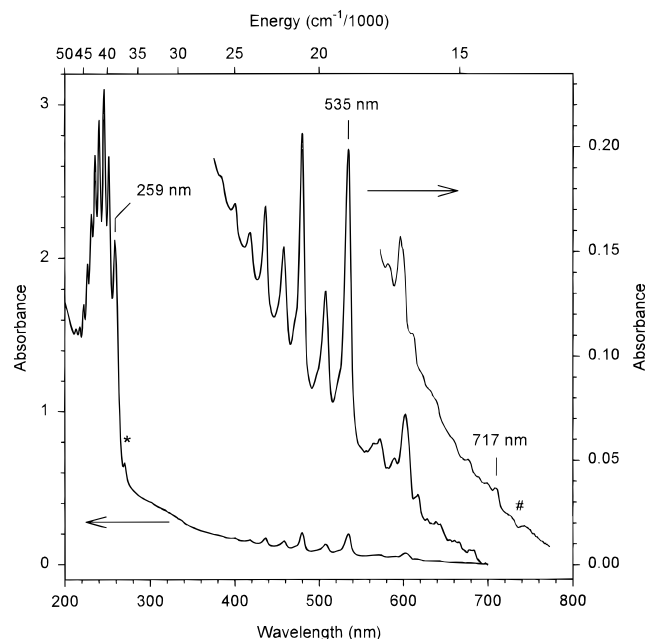


**Figure 1.** Electronic absorption spectrum of propadienylidene (**1**) obtained upon irradiation ( $\lambda > 472$  nm, 22.5 h;  $\lambda > 261$  nm, 7.5 h) of diazopropane, matrix isolated in argon at 10 K. Inset (600–780 nm) obtained from an independent experiment. (\* = singlet cyclopropenylidene; # = instrumental artifact.)

**Table 1.** Adiabatic Excitation Energies and Harmonic Vibrational Frequencies Calculated for Propadienylidene (**1**) Using the EOMEE-CCSD Method<sup>a</sup>

	$\tilde{A}^1A_2$	$\tilde{B}^1B_1$	$\tilde{C}^1A_1$
TZ2P	1.836	2.507	5.321
cc-pVTZ	1.851	2.516	5.369
cc-pVQZ	1.853	2.520	5.350
expt	<1.73	2.32 ± 0.01	4.79 ± 0.04
CC stretch	1701.4	2125.9	1546.0
	1068.4	1068.7	1001.4

<sup>a</sup> Energies in eV, frequencies (TZ2P basis) in  $\text{cm}^{-1}$ ; calculations performed on TZ2P equilibrium geometries.

Table 1 are within 0.1 eV of the basis set limit EOMEE-CCSD adiabatic excitation energies.

Two distinct band systems with relatively long vibrational progressions can be seen in Figure 1, a low-energy transition that lies primarily in the visible (from 535 to 382 nm) and a strong UV absorption that begins at 259 nm and extends to 213 nm. In addition, there are some weak and irregularly spaced features at wavelengths beyond 550 nm which appear to be due to **1**. Both the intensity pattern and the regular nature of the spacing in the high-energy progression starting at 259 nm are suggestive of a single Franck–Condon active mode with an upper state frequency of *ca.* 900  $\text{cm}^{-1}$ . Spacings between absorptions in the 535-nm-band system are relatively consistent (*ca.* 1000  $\text{cm}^{-1}$ ), but the intensity pattern is more complicated than that seen in the higher energy feature. Notably, the third peak in the band system is nearly as strong as the apparent 0–0 band, and much stronger than the feature that lies between them.

Given the resolved nature of the two unambiguous band systems, corresponding 0–0 transitions can be assigned to features at 535 and 259 nm with some confidence. The corresponding adiabatic excitation energies are  $2.32 \pm 0.01$  and  $4.79 \pm 0.04$  eV, where a wavelength uncertainty of 2 nm has been assumed. The former value is roughly 0.20 eV below the value obtained for the  $\tilde{B}^1B_1$  state at the EOMEE-CCSD level with the cc-pVQZ basis; somewhat poorer agreement exists between the theoretical value of 5.350 eV for the  $\tilde{C}^1A_1 \leftarrow \tilde{X}^1A_1$

transition and the apparent origin of the short wavelength band system. The discrepancy between calculated and theoretical adiabatic transition energies for the latter is somewhat larger in magnitude than found in previous EOMEE-CCSD calculations,<sup>12,15</sup> suggesting that higher-order correlation effects are important for the  $\tilde{C}^1A_1$  state. The zero-point level of the first excited state ( $\tilde{A}^1A_2$ ) is predicted to lie approximately 1.9 eV above the ground state, corresponding to a photon wavelength of about 670 nm. However, the  $\tilde{A}^1A_2 \leftarrow \tilde{X}^1A_1$  transition is only vibronically allowed, which explains why no well-defined band system is seen. It is probable that the features seen at wavelengths beyond 535 nm are due to transitions to levels of  $\tilde{A}^1A_2$  with  $^1A_1$ ,  $^1B_1$ , and  $^1B_2$  vibronic symmetry. The lowest energy feature in this region of the spectrum is found at 717 nm (1.73 eV), which provides an upper bound to the adiabatic excitation energy. While this is clearly consistent with the theoretically predicted energy difference, further experimental work is warranted before a definitive vibronic assignment of this region of the spectrum can be made.

Additional support for assignment of the 535- and 259-nm-band systems to the  $\tilde{B}^1B_1 \leftarrow \tilde{X}^1A_1$  and  $\tilde{C}^1A_1 \leftarrow \tilde{X}^1A_1$  electronic transitions of **1** comes from the predicted excited state geometries and harmonic vibrational frequencies. For  $\tilde{C}^1A_1$ , the geometry change that accompanies excitation is almost entirely along the in-phase C–C stretching normal coordinate; displacements along both C–C stretching modes dominate the difference between equilibrium geometries of the  $\tilde{X}^1A_1$  and  $\tilde{B}^1B_1$  states.<sup>21</sup> The progressions seen in the 259-nm-band system are clearly consistent with the calculations, as the predicted in-phase C–C stretching frequency of 1001  $\text{cm}^{-1}$  is probably above the true fundamental due to neglect of anharmonicity. The intensity pattern observed in the visible absorption feature can be rationalized as follows. Frequencies predicted for the two C–C stretching modes differ by almost exactly a factor of 2, so (to zeroth-order) transitions to vibrational levels of the upper state with  $2n$  quanta in the lower frequency mode will be nearly degenerate with those having  $n$  quanta in the higher frequency mode. Therefore, the prominence of the third peak in the absorption feature relative to the origin may be attributed to the probability that two distinct vibronic transitions contribute to its intensity. A more quantitative analysis of this band system necessarily requires consideration of vibrational state resonances and Duschinsky mixing and is beyond the scope of this work. Nevertheless, the EOMEE-CCSD calculations are qualitatively consistent with assignment of the 259- and 535-nm-band systems to  $\tilde{C}^1A_1 \leftarrow \tilde{X}^1A_1$  and  $\tilde{B}^1B_1 \leftarrow \tilde{X}^1A_1$  transitions of **1**. A discussion of the electronic structure of the upper states and their role in the mechanism of the observed photochemical automerization of **1** will be reported in a separate publication.

**Acknowledgment.** This work was supported by the Robert A. Welch Foundation (J.F.S.), the Alfred P. Sloan Foundation (J.F.S. and R.J.M.), the Petroleum Research Fund administered by the American Chemical Society (J.F.S. and R.J.M.), and the National Science Foundation (Young Investigator Award to J.F.S.; Graduate Fellowship to R.A.S.; Grant CHE-9301025 to R.J.M.). We are grateful to J. Gauss (Mainz) for a critical reading of the manuscript.

**Supporting Information Available:** Table containing computed geometries and vibrational frequencies (1 page). See any current masthead page for ordering and Internet access instructions.

JA961900B

(21) The totally symmetric normal coordinates for the C–C stretching modes differ appreciably (Duschinsky effect) for the  $\tilde{X}^1A_1$  and  $\tilde{B}^1B_1$  electronic states; a Franck–Condon analysis of the spectrum based on the parallel mode approximation is therefore unreliable. Nevertheless, the geometry change is dominated by these modes. The picture is much simpler for the  $\tilde{C}^1A_1$  state, where the geometry change is almost entirely along low-frequency C–C stretching mode and the extent of mode mixing is negligible.